Diagnostic Accuracy Study

Medicine®

OPEN

The capsule appearance of hepatocellular carcinoma in gadoxetic acid-enhanced MR imaging

Correlation with pathology and dynamic CT

Bohyun Kim, MD[a], Jei Hee Lee, MD[a,*], Jai Keun Kim, MD[a], Hye Jin Kim, MD[a], Young Bae Kim, MD[b], Dakeun Lee, MD[b]

Abstract

This study aimed to evaluate the capability of gadoxetic acid-enhanced MR (GAeMR) to detect presence of capsule appearance in hepatocellular carcinoma (HCC), and to correlate it with dynamic computed tomography (CT) and pathological features.

Sixty-three patients (54: 9=M: F, mean age 55.8) surgically confirmed HCCs with preoperative CT and GAeMR were included in this retrospective study. Two readers evaluated presence of capsule appearances on CT and GAeMR images in each phase including precontrast (Pre), portal phase (PP), delayed phase (DP), transitional phase (TP), and hepatobiliary phase (HBP). Histologic capsule was compared with CT and GAeMR. Diagnostic performance of CT and GAeMR of each phase for histologic capsule was evaluated and compared by receiver operating characteristic curve. Interobserver agreement was assessed with kappa statistics.

Histologically the capsule was complete in 12.7% (8/63) and incomplete in 60.3% (38/63). Four cases (6.3%) were pseudocapsule. Interobserver agreement for capsule appearance on GAeMR was good in Pre ($\kappa = 0.684$), moderate in PP ($\kappa = 0.434$), poor in TP ($\kappa = 0.187$), fair in HBP ($\kappa = 0.395$), and moderate on CT in PP ($\kappa = 0.476$) and DP ($\kappa = 0.485$). Diagnostic performance and sensitivity for the histologic capsule in DP on CT was highest among PP on CT and other phases on GAeMR. DP on CT images showed a higher Az value than PP on CT images with statistical significance ($P < .001$). PP on MR images revealed higher Az value than PP on CT images.

The capsule appearance was most frequently observed in the DP on CT with highest diagnostic performance, and so DP images should be obtained on CT study for liver mass categorization. GAeMR yielded comparable capsule appearance to CT with moderate interobserver agreement. Considering hypointense rim on the HBP as fibrous capsule on pathology should be refrained, and so further study is warranted to correlate HBP hypointense rim with pathologic findings.

Abbreviations: AP = arterial phase, CT = computed tomography, DP = delayed phase, ECCA = extracellular contrast agent, FC = fibrous capsule, GAeMR = gadoxetic acid-enhanced MR, HBP = hepatobiliary phase, HCC = hepatocellular carcinoma, HU = Hounsfield Unit, LI-RADS = Liver Imaging Reporting and Data System, MR = magnetic resonance, PP = portal phase, Pre = precontrast, TP = transitional phase.

Keywords: capsule appearance, CT, gadoxetic acid-enhanced MR, hepatocellular carcinoma

1. Introduction

Hepatocellular carcinoma (HCC) is the most common primary liver cancer, and to date the third most common cause of cancer deaths worldwide.[1,2] Typical HCC reveal rapid enhancement in the arterial phase (AP) and portal phase (PP) or delayed phase (DP) washout in contrast-enhanced computed tomography (CT) and magnetic resonance (MR) imaging.[3]

The presence of a capsule appearance is considered as favorable prognostic factor of HCC.[4,5] Capsule appearance is a peripheral rim of smooth hyperenhancement surrounding background nodules in the PP and DP in contrast-enhanced CT and MR, and has been regarded as histological fibrous capsule (FC) or pseudocapsule.[5,6] Presence and recognition of a capsule appearance is crucial for noninvasive diagnosis of HCC, and Liver Imaging Reporting and Data System (LI-RADS) included capsule appearance as a major imaging feature.[7,8]

Gadoxetic acid disodium, with properties of extracellular and hepatocyte-specific contrast agent, enables dynamic and hepatobiliary phase (HBP) imaging.[1,9,10] Washout or capsule appearance on PP and DP on extracellular contrast agent (ECCA)-enhanced CT or MR images are different from those on gadoxetic acid-enhanced MR (GAeMR) images.[9,10]

There are limited studies evaluating capsule appearance of HCC on GAeMR.[8,11–13] The purpose of this study was to evaluate the capability of GAeMR imaging to detect presence of

Editor: Neeraj Lalwani.

Funding: This work was supported by the Central Medical Service, Seoul, South Korea (grant number GA104-04).

The authors have no conflicts of interest to disclose.

[a] Department of Radiology, [b] Department of Pathology, Ajou University School of Medicine, Suwon-si, Republic of Korea.

[*] Correspondence: Jei Hee Lee, Department of Radiology, Ajou University School of Medicine, 164, World cup-ro, Yeongtong-gu, Suwon-si, Gyeonggi-do 16499, Republic of Korea (e-mail: radljh@ajou.ac.kr).

Medicine (2018) 97:25(e11142)

Received: 24 January 2018 / Accepted: 23 May 2018

http://dx.doi.org/10.1097/MD.0000000000011142

the capsule appearance in HCC including HBP, and to correlate it with dynamic CT and pathological findings.

2. Materials and methods

2.1. Patient se2lection

The institutional review board approved this retrospective study and the requirement for informed consent was waived. Patients that underwent preoperative GAeMR and dynamic CT January 2013–December 2015 were included for analysis. Patients that had undergone preoperative transarterial chemoembolization, hepatic arterial infusion chemotherapy, and systemic chemotherapy were excluded. We included the largest HCC per patient to avoid cluster effect in statistical analysis. Sixty-three patients were pathologically confirmed HCCs after surgical resection (wedge resection: 18, segmentectomy: 15, sectionectomy: 14, hemihepatectomy: 13, extended hemihepatectomy: 1, total hepatectomy: 2).

There were 54 men (mean age, 55.3, 55.3 ± 9.5; age range, 36–78) and 9 women (mean age, 59.2, 59.2 ± 9.0; age range, 44–72).

Underlying causes of cirrhosis (as determined from available pathological/laboratory data and hepatology clinical notes) included viral hepatitis B (n = 52), viral hepatitis C (n = 3), alcohol abuse (n = 4), and others (n = 5).

2.2. Image acquisition

CT was conducted by using one of the following CT scanners: Sensation 16 (Siemens Healthcare, Forchheim, Germany) (n = 10), SOMATOM Definition Flash (Siemens Healthcare) (n = 22), Brillance 16 (Philips Healthcare, Cleveland, OH) (n = 11), or Brillance 64 (Philips Healthcare) (n = 20).

Precontrast CT scans were obtained before contrast media injection. A total of 120 to 150 mL (2 mL/kg) of a nonionic contrast material (iohexol [Bonorex 350, Central Medical Service, Seoul, South Korea] and iopamidol [Iopamiro 300, Bracco, Milan, Italy]) was injected into an antecubital vein through an 18-gauge plastic intravenous catheter. Hepatic AP were obtained with a scan delay of 18 seconds after the Hounsfield Unit (HU) of the abdominal aorta reached 100 HU with a power injector at a rate of 3 mL/s. PP and DP images were obtained at 75 to 85 and 180 to 190 seconds after contrast injection. CT scans were obtained at a tube current-time product of 150 to 200 mAs and a peak voltage of 120 kVp. Whole-liver scanning was completed in 4 to 8 seconds while patients held their breath. Images were reconstructed with a 5-mm slice thickness. The time interval between the examination of CT and examination of MRI was less than 1 month except three patients (median 12 days).

All MRI studies were conducted with a 1.5-T system (Signa HDxt; GE Healthcare, Milwaukee, WI) with phased array coils. All MR images were acquired in the axial plane. MR protocol consisted of a dual-echo T1-weighted gradient-echo sequence (in-phase and opposed-phase), a respiratory-triggered fast spin T2-weighted sequence, and a contrast-enhanced dynamic sequence using a T1-weighted 3D gradient-echo sequence with fat-suppression. Parameters for all sequences are presented in Table 1. For contrast-enhanced dynamic and HBP MR images, Gd-EOB-DTPA was administered at 0.025 mmol per kilogram of body weight at 1 mL per second, followed by a 20-mL saline flush. Imaging of the AP was performed 8 seconds after contrast agent arrival at the left ventricle of the heart by the use of an automated triggering technique (SmartPrep, GE Healthcare). After administering contrast, AP (25–30 seconds), PP (60 seconds), TP (3 minutes), and additional HBP (after 20 minutes) images were obtained.

2.3. Image analysis

Preoperative CT and GAeMR images were retrospectively analyzed on a picture archiving and communication system (Infinitt PACS, version 3.0; Infinitt Healthcare, Seoul, Korea).

Two board-certified abdominal radiologists qualitatively evaluated CT and MR images. And finally, discrepancies between the 2 readers were resolved by discussion to reach consensus. Readers were aware that patients had undergone liver surgery and that pathologic reports confirmed HCC, but they were blinded to all other clinical, laboratory, and pathologic details.

Each reader evaluated presence or absence of capsule appearance on CT and GAeMR. Capsule appearance was defined according to the LI-RADS lexicon, and applies to observations that have a peripheral rim of smooth hyperenhancement that is thicker or more conspicuous than rims surrounding background nodules in the PP and DP. And we used same way in TP on GAeMR. Presence or absence of capsule appearances on CT and GAeMR images were analyzed in the PP and DP/TP. Hypointense rims on T1- and T2 weighted images were considered as capsule on precontrast (Pre). Smooth hypointense rims surrounding background nodules in HBP were considered as capsule appearance on HBP in GAeMR.[6,13] Peripheral AP enhancement and temporal reduction in enhancement of the periphery of the lesion relative to the liver was regarded as peripheral washout appearance, which favors other malignancies such as cholangiocarcinoma.[13,14] Irregular circumferential enhancement around HCC in AP or PP was regarded as transient peritumoral enhancement or corona enhancement.[15] Peripheral washout, peritumor enhancement, and corona enhancement shows irregular and nonsmooth appearance, but capsule appearance is smooth.

2.4. Histopathologic examination

An expert pathologist that has specialized in liver pathology examined all the cases. For gross and histological examinations, clinical and imaging data were freely accessible in electronic

Table 1

MR imaging sequences and parameters.

Parameters	TR/TE, ms	Flip angle, degree	Section thickness, mm	Intersection gap, mm	Matrix size	Reduction factor
Double-echo T1-weighted gradient echo	6.2/2.0–4.1	12	2.5	0	288 × 192	1.74
Single shot heavily T2 weighted	900–1100/160	90	7	1	380 × 380	2
Respiratory-triggered fast-spin T2-weighted	7000–8000/84	90	7	1	320 × 224	1
T1-weighted 3D gradient echo	4.2/2.0	12	2.5	0	361 × 380	1.73

3D = three-dimensional, TE = echo time, TR = repetition time.

medical records and through a picture archiving and communication system. However, the diagnosis of each lesion was solely based on histological features.

Pathologists classified gross subtype as one of the following: vaguely nodular type; nodular expanding, with the gross appearance of a clear round nodule; nodular with perinodular growth, with gross appearance similar to the nodular expanding type and exhibited varying degrees of extranodular growth; multinodular confluent, which had the appearance of a nodule comprised of a cluster of small and confluent nodules; or infiltrative.[16]

Histopathologic features of tumors, degree of tumor differentiation (Edmondson-Steiner grade), degree of liver fibrosis, and presence of microvascular invasion were recorded. FC formation was recorded as present or absent, and if present, was divided into partial (<90% of the tumor circumference) or complete (≥90%). Pseudocapsule at imaging was defined as HCC that revealed capsule appearance on dynamic images despite being negative for histologic FC (false-positive FC cases)

2.5. Statistical analysis

Significant differences were defined as those with $P < .05$. All statistical analyses were conducted using MedCalc Statistical Software version 17.5.5 (MedCalc Software bvba, Ostend, Belgium; http://www.medcalc.org; 2017).

Histologic FC was compared with histopathologic features of tumors, degree of tumor differentiation, degree of background liver fibrosis, gross morphologic type, and presence of microvascular invasion using χ^2 test.

Interobserver agreement was assessed with kappa statistics, and consensus opinions were reached by conference. Interobserver agreement of categorical data was evaluated using Cohen's kappa statistic. The κ values were interpreted as poor for κ less than 0.20; fair, κ of 0.21 to 0.40; moderate, κ of 0.41 to 0.60; good, κ of 0.61 to 0.80; and very good, κ of 0.81 to 1.00.

Histologic FCs were compared and correlated with CT and GAeMR. And sensitivity, specificity, and accuracy were calculated. The diagnostic performance of CT and GAeMR and each phase for diagnosis of histologic FC was evaluated by calculating the area under the receiver operating characteristic curve (Az) and compared in terms of Az values.

3. Results

The median diameter of the tumor was 2.70 cm (mean diameter = 3.57, standard deviation 2.98 cm, range 1.0–18 cm). The capsule was histologically evident in 46 of 63 nodules (73.0%), complete in 8 (12.7%), and incomplete in 38 (60.3%) (Fig. 1). Four cases (6.3%) were pseudocapsule (Fig. 2) with false-positive FC on CT and GAeMR images.

The characteristics of 63 patients with HCCs are summarized in Tables 2 and 3. Histological FC was not correlated to size of the HCC ($P = .64$) (Tables 3 and 4), stage of fibrosis ($P = .70$), and etiologic factors of hepatitis or cirrhosis ($P = .63$). To the contrary, a relationship was found between the degree of tumor differentiation ($P = .04$) and microvessel invasion ($P < .05$). FC was more frequent in Grade I or II differentiation and in absence of microvessel invasion. Gross type of HCC reveals statistical significance ($P < .001$) and FC was more common in expanding nodular type or nodules with perinodular extension type.

Interobserver agreement for presence or absence of capsule appearance on GAeMR was good in Pre (κ = 0.684), moderate in PP (κ = 0.434), poor in TP (κ = 0.187), and fair in HBP (κ = 0.395). Interobserver agreement for capsule appearance on CT was moderate in PP (κ = 0.476) and DP (κ = 0.485) (Table 5).

Correlation between histologic FC and presence of capsule appearance on each phases of CT and GAeMR are summarized in Tables 6 and 7. Comparison between the stage of fibrosis in background liver with capsule appearance on GAeMR is summarized in Table 8. There was statistical significance between the degree of fibrosis in the background liver and detection of capsule appearance on HBP ($P = .032$) (Table 8).

Diagnostic performance, including mean Az values, sensitivities, specificities, and accuracy for presence of histologic FC on CT and GAeMR images are summarized in Table 9. DP on CT images showed a higher Az value than PP on CT images with statistical significance ($P < .001$). PP on MR images revealed higher Az value than PP on CT images. Overall MR imaging revealed a slightly lower Az value than those of CT imaging and differences were not statistically significant ($P = .74$). Sensitivity and accuracy for the diagnosis of FC in DP was higher than PP on CT.

4. Discussion

FC formation was frequently (46 of 63 nodules, 73.0%) seen in the HCCs in our study. Encapsulated HCCs are considered to have a favorable prognosis because they tend to have a lower incidence of direct liver invasion, fewer tumor microsatellites, and less vascular invasion than nonencapsulated HCCs.[4,17] However, with improvements in CT and in MR imaging technology for detection of hepatic nodule and widespread use of cross-sectional imaging, imaging plays a critical role in diagnosis of HCC, and diagnosis of HCC can be achieved by noninvasive imaging with typical imaging features.[3] Capsule appearance on imaging is highly specific for diagnosis of HCC,[18,19] and it is one of the critical imaging criteria in LI-RADS and the Organ Procurement and Transplantation Network for the noninvasive diagnosis of HCC.[7,8]

Pathogenesis of FC formation could be attributed either to a passive thickening of liver stroma under expansion pressure of the tumor or to a defense mechanism deployed by surrounding parenchyma to restrain the tumor nodule that causes a mechanical insult to adjoining tissues.[20] Based on our results, presence of histologic FC reveals the relationship between the lower Edmondson-Steiner grade, absence of microvessel invasion, and gross type of HCC with expanding nodular type or nodular with perinodular extension type. In our study, the degree of liver fibrosis in the background liver does not correlate with HCC with histologic FC ($P = .70$). There was statistical significance between the degree of fibrosis in the background liver and detection of capsule appearance on HBP ($P = .032$). So, the detection of capsule appearance on HBP was difficult in severe degree of fibrosis in the background liver. But, Ishigami et al[5] described the degree of fibrosis in the background liver was more severe in HCCs with histologic FC than in those with a pseudocapsule. Although the mechanism for formation of FC is unclear, there was a report that activated stellate cells played an important role in the development of liver fibrosis.[21]

The degree of liver parenchymal enhancement was correlated with liver function in GAeMR, and Child–Pugh classifications also showed a significant correlation with the liver enhancement on HBP images.[22] Recognition of the capsule appearance on HBP might be affected by background liver enhancement in GAeMR. But, in our study, all patients were surgically confirmed,

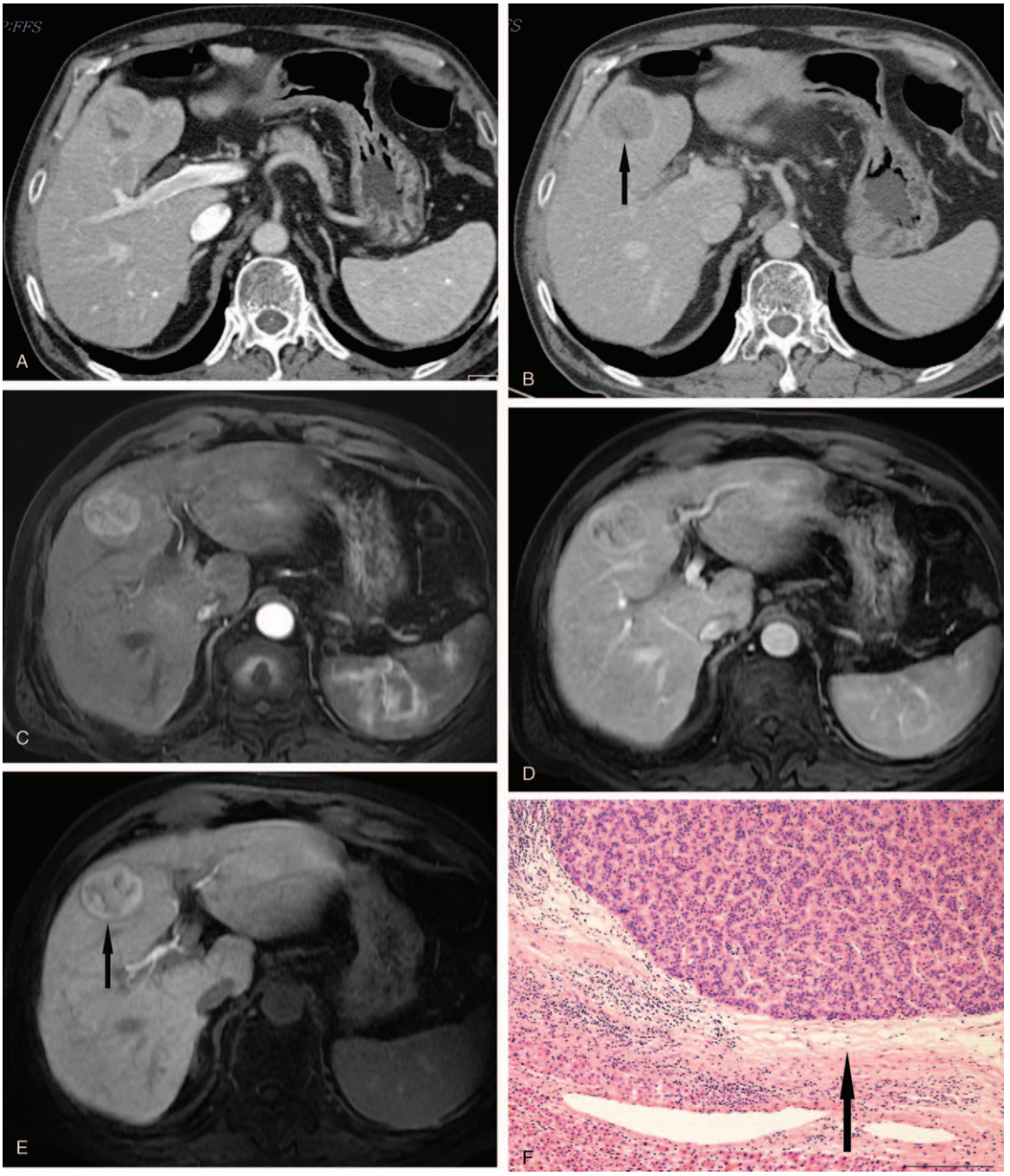

Figure 1. A 71-year-old man with HCC with histologic fibrous capsule. Portal (A) and delayed (B) phase CT image reveals mass with washout appearance. Peripheral rim of smooth hyperenhancing capsule appearance (arrow) is seen on delayed phase. (C) Arterial phase MR image shows hypervascular mass lesion. (D) Portal phase MR image shows hyperintense rim around tumor. (E) Hepatobiliary phase MR image shows hypointense (arrow) rim around tumor. (F) Pathologic specimen shows thick fibrous capsule (arrow).

and 96.8%(61/63) patients were Child–Pugh class A and only 2 cases were Child–Pugh class B, and so, all of the HBP images showed acceptable hepatic parenchymal enhancement.

Capsule appearance on imaging does not always represent a true tumor capsule and may instead represent a pseudocapsule.[13] Capsule appearance in HCC, either histologic FC or pseudocapsule, reveals on imaging in 43% to 64% of cases.[5,8,18] Ishigami et al[5] reported that approximately 14% of HCCs (15 of 106) revealed pseudocapsule, an enhancing rim in the DP of dynamic MR despite being negative for histologic FC. In our study, 4 cases (6.3%) were considered as pseudocapsule with false-positive FC on CT and GAeMR images. The difference between 2 studies originated from the difference in pharmacokinetics of GAeMR and ECCA-enhanced MR and selection bias. At histopathologic examination, a pseudocapsule possibly reflected prominent sinusoids and/or peritumoral fibrosis.[5] When peritumoral fibrosis and prominent sinusoids coexisted, peritumoral fibrosis was typically observed at the inner layer.[5]

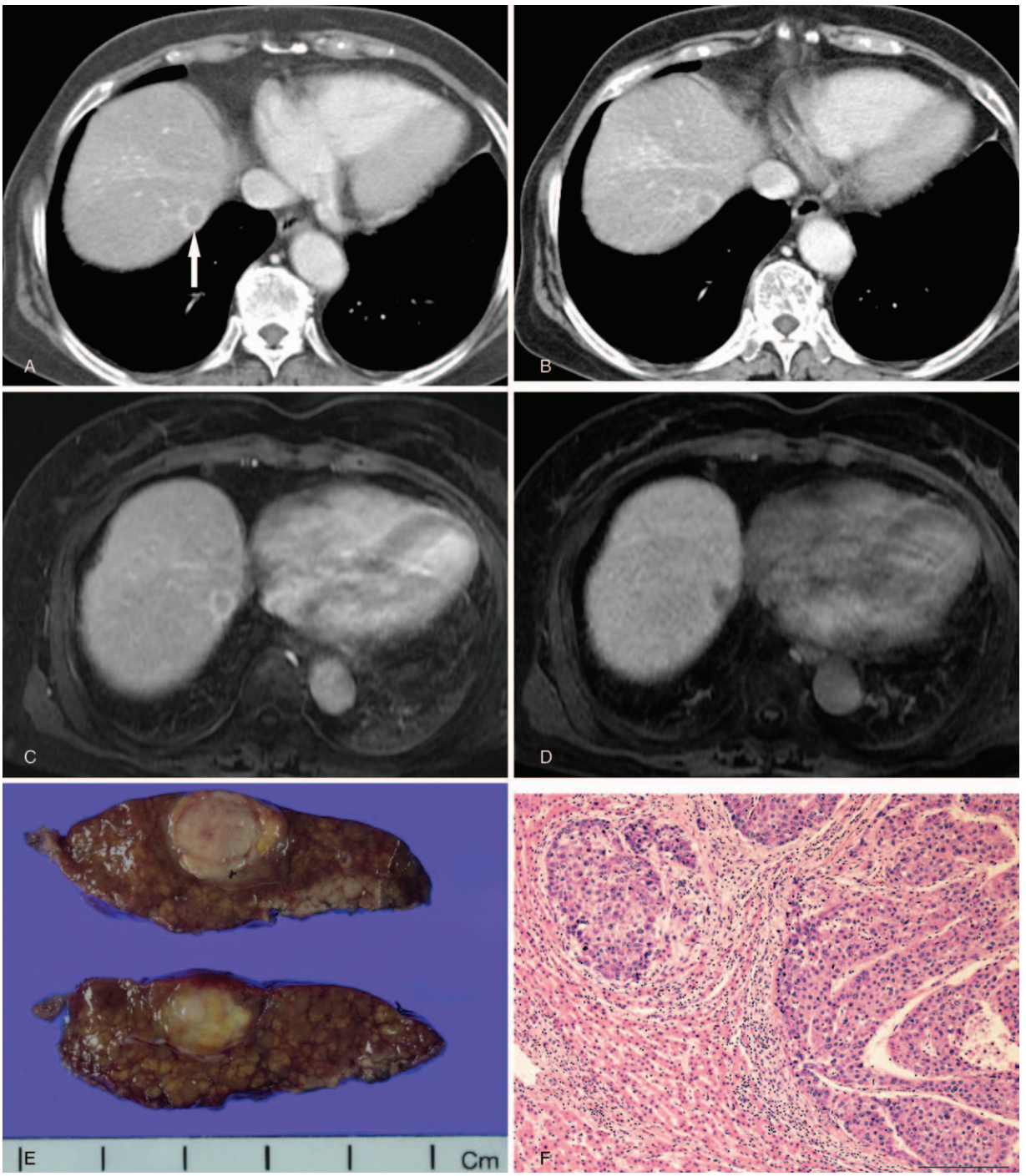

Figure 2. A 73-year-old woman with HCC with pseudocapsule. Portal (A) and delayed (B) phase CT image shows mass with peripheral rim of smooth hyperenhancing capsule appearance (arrow). (C) Portal phase MR image shows mass with peripheral rim of smooth hyperenhancing capsule appearance. (D) Hepatobiliary phase MR image shows hypointense mass without capsule appearance. Gross (E) and microscopic (F) pathologic specimen shows no fibrous capsule.

Thickness of the pseudocapsule was not significantly different from combined thickness of histologic FC and prominent sinusoids.[5] Despite the different histologic appearances, histoloigic FC and pseudocapsule are similar on imaging and have high positive predictive value for HCC in at-risk patients.[12]

In ECCA-enhanced MRI, fibrotic tissue typically reveals progressive enhancement, due to accumulation of gadolinium in the extracellular interstitial spaces.[6] However, in GAeMR, fibrosis is hypointense on HBP due to lack of hepatocytes in fibrotic tissue and to faster clearance of this contrast agent from extracellular space.[8] Capsule appearance may be more difficult to appreciate on TP or HBP due to enhancement of the background liver parenchyma.[12,15] Therefore, capsule appearance is likely more reliably visualized with ECCA than

Table 2

Characteristics of 63 patients with HCCs.

Characteristics	Datum
Age (mean years)	
Male/female	55.3/59.2
Sex	
Male/female	54/9
Etiology of liver disease	
HBV/HCV/alcoholic/others	51/3/4/5
Child–Pugh class	
A/B/C	61/2/0

HBV = hepatitis B virus, HCV = hepatitis C virus.

Table 3

Histopathologic features of 63 HCCs and correlation with presence of histologic fibrous capsule.

Characteristics	Datum	*P*
Fibrous capsule formation		
Absence/partial/complete	17/38/8	
Size, cm		$P = .64$
<2	15	
2–3	18	
3–5	21	
≥5	9	
Gross subtype		$P < .01$*
Vaguely nodular type	4	
Nodular expanding	24	
Nodular with perinodular growth	22	
Multinodular confluent	6	
Infiltrative	7	
Edmondson–Steiner grade		$P = .04$*
1/2/3/4	13/22/25/4	
Stage of liver fibrosis		$P = .70$
0/1/2/3/4	3/4/24/1/31	
Microvascular invasion		$P < .05$*
Absence/presence	40/23	

Categorical variables were compared with histologic fibrous capsule using χ^2 test.
* Statistical significance with histologic fibrous capsule.

hepatobiliary agents.[12,15] In our study, GAeMR in PP yielded better capsule appearance than GAeMR in TP and HBP. And CT in DP yielded significantly better capsule appearance than CT in PP. But, overall GAeMR yielded comparable capsule appearance to CT. Kim et al[23] reported similar result to our study, and that ECCA-enhanced MRI yielded significantly better capsule appearance in HCC than CT and GAeMR in PP and DP/TP, but there was no significant difference between CT and GAeMR.

Table 5

Interobserver agreement of capsule appearance on CT and GAeMR.

Imaging	Kappa value
CT PP	0.476 (0.249, 0.704)
CT DP	0.485 (0.274, 0.695)
MR PP	0.434 (0.251, 0.616)
MR TP	0.187 (0.078, 0.453)
MR HBP	0.395 (0.140, 0.650)
MR pre	0.684 (0.510, 0.858)

Data are κ statistics. Data in parentheses are 95% confidence intervals.
CT = computed tomography, DP = delayed phase, HBP = hepatobiliary phase, MR = magnetic resonance, PP = portal phase, Pre = precontrast, TP = transitional phase.

But, Dioguardi Burgio et al[8] reported that capsule appearance was detected in GAeMR in PP (24%), TP (15%), and HBP (17%). The much lower prevalence of capsule appearance was the selection bias by HCC with typical imaging features in cirrhosis.[8] There is significant discordance between CT and MR for assignment of major LI-RADS features, and the capsule appearance was observed more frequently at ECCA-enhanced MRI than CT.[7,24] However, Joo et al[25] reported that the capsule appearance was less frequently observed on GAeMR than on CT (PP and DP), but Hope et al[26] reported that the capsule appearance were less frequently observed on CT (PP only) than GAeMR. Discrepancy in the capsule appearance observed between CT and GAeMR is likely underestimating the value of DP on CT.[11,25,26] Diagnostic performance and sensitivity for diagnosis of FC in DP on CT was highest compared to PP on CT and other phases on GAeMR. So, DP images should be obtained on CT for liver mass evaluation. But, overall MR imaging revealed comparable diagnostic performance for histologic FC detection with CT.

Davenport et al[27] reported that interobserver reliability for individual imaging features is variable, with high agreement in AP hyperenhancement at gadobenate dimeglumine-enhanced MR, but poor agreement on washout or capsule appearance. But most of the interobserver reliability study for HCC reveals moderate to substantial agreement for capsule appearance on CT and MR.[7,24,25,28] Chernyak et al[11] reported that the interobserver agreement between CT and GAeMR was fair to moderate for capsule appearance. And, however, the interobserver agreement between the readers was almost perfect for capsule on CT, but moderate on GAeMR.[11] In our study, interobserver agreement for the capsule appearance was moderate on CT in PP and DP. And that was moderate in PP on GAeMR, but poor in TP and fair in HBP. Because of background parenchymal enhancement may obscure capsule appearance during the TP or HBP and variable

Table 4

Comparison between the diameter of the HCC and histological capsule, capsule on CT, and capsule on GAeMR.

	Histological Capsule			Capsule on CT		Capsule on MR		
Size, cm	No capsule	Partial	Complete	Absent	Present	Absent	Present	Total
<2	4	11	0	10	5	8	7	15
2–3	5	9	4	8	10	9	9	18
3–5	5	13	3	5	16	4	17	21
≥5	3	5	1	3	6	3	6	9
Total (N = 63)	17	38	8	26	37	24	39	63

CT = computed tomography, GAeMR = gadoxetic acid-enhanced MR, MR = magnetic resonance.

Table 6

Comparison between the pathological capsule and CT findings.

	Capsule on CT (consensus)		Capsule on CT (PP)		Capsule on CT (DP)	
Histological capsule	Absent	Present	Absent	Present	Absent	Present
No capsule (n=17)	13	4	14	3	13	4
Partial capsule (n=38)	12	26	24	14	15	23
Complete capsule (n=8)	1	7	5	3	1	7
Total (N=63)	26	37	43	20	29	34

CT=computed tomography, DP=delayed phase, PP=portal phase.

Table 7

Comparison between the pathological capsule and GAeMR findings.

	Capsule on MR (consensus)		MR (PP)		MR (TP)		MR (HBP)		MR (Pre)	
Histological capsule	Absent	Present	Absent	Present	Absent	Present	Absent	Present	Absent	Present
No capsule (n=17)	12	5	13	4	14	3	14	3	14	3
Partial capsule (n=38)	12	26	15	23	27	11	23	15	19	19
Complete capsule (n=8)	0	8	3	5	3	5	4	4	0	8
Total (N=63)	24	39	31	32	44	19	41	22	33	30

GAeMR=gadoxetic acid-enhanced MR, HBP=hepatobiliary Phase, MR=magnetic resonance, PP=portal phase, Pre=precontrast, TP=transitional phase.

Table 8

Comparison between the stages of fibrosis in the background liver in HCCs with capsule appearance on GAeMR.

	MR (PP)		MR (TP)		MR (HBP)		MR (Pre)	
Fibrosis stage	Absent	Present	Absent	Present	Absent	Present	Absent	Present
0	2	1	2	1	1	2	1	2
1	2	2	2	2	3	1	3	1
2	16	8	19	5	17	7	11	13
3	1	0	1	0	1	0	1	0
4	23	8	23	8	27	4	17	14
Total (N=63)	44	19	47	16	49	14	33	30
P	.377		.732		.032*		.648	

GAeMR=gadoxetic acid-enhanced MR, HBP=hepatobiliary phase, MR=magnetic resonance, PP=portal phase, Pre=precontrast, TP=transitional phase.
* Statistical significance with histologic fibrous capsule.

degree of parenchymal enhancement in HBP by liver function can lead to greater interobserver variability.[1,12,15] Additionally, reader perception of capsule appearance was affected by washout appearance, like the Mach band effect.[29] Imaging features of washout on GAeMR can be exaggerated by delayed parenchymal enhancement from hepatocellular uptake of gadoxetic acid, which is called "pseudo washout" effect.[10]

Table 9

Diagnostic performance of pathological capsule on CT and GAeMR.

Imaging	Az value	Sensitivity (%)	Specificity (%)	Accuracy (%)
CT total	0.756	71.74	76.47	73.02
CT PP	0.561	36.96	82.35	49.21
CT DP	0.724	65.22	76.47	68.25
MR total	0.746	73.91	70.59	73.02
MR PP	0.626	60.87	76.47	68.08
MR TP	0.593	34.78	82.35	47.62
MR HBP	0.652	41.30	82.35	52.38
MR Pre	0.705	58.70	82.35	65.08

CT=computed tomography, DP=delayed phase, GAeMR=gadoxetic acid-enhanced MR, HBP=hepatobiliary phase, MR=magnetic resonance, PP=portal phase, Pre=precontrast, TP=transitional phase.

Smooth hypointense rim surrounding nodules in HBP images were considered as capsule appearance in our study. Hypointense capsule appearance on the HBP in the 2014 version of LI-RADS (defined as a "hypointense rim on the HBP") is considered a new ancillary feature favoring malignancy.[8,28] In the 2017 version of LI-RADS, nonenhancing capsule, defined as a capsule appearance that is not depicted as an enhancing rim, is considered an ancillary feature that favors HCC.[14] Hypointense rim on the HBP can be considered as FC, corresponding to capsule appearance on PP and DP with ECCA.[8,28] An et al[13] proposed using smooth hypointense rim in HBP in addition to conventional PVP capsule appearance in GAeMR. But in our study, sensitivity for histologic FC on GAeMR in HBP was low and interobserver agreement was fair. So considering hypointense rim on the HBP as FC on pathology should be refrained.

Our study had several limitations. First, due to the retrospective design of this study, patient selection bias may have been present. We included only surgically confirmed HCC cases to

compare CT and GAeMR imaging with histological characteristics. Therefore, our study did not include small HCCs that were diagnosed based on typical dynamic patterns, and patients that did not have surgical indications such as HCCs in advanced cirrhosis with decreased liver function. Secondly, our study was conducted in an institution and was limited by relatively small sample size. There may have been a potential bias among readers when reviewing CT and MR images, surgeons and pathologist in clinical practice. Thirdly, pathologic analysis was based on pathology reports without reexamination of pathologic slides. So, radiologic–pathologic correlation could not be assessed for all cases.

5. Conclusions

In conclusion, the capsule appearance was most frequently observed in the DP on CT with highest diagnostic performance, and so DP images should be obtained on CT study for liver mass categorization. GAeMR yielded comparable capsule appearance on CT with moderate interobserver agreement. Considering hypointense rim on the HBP as FC on pathology should be refrained, and so further study is warranted to correlate HBP hypointense rim with pathologic findings.

Author contributions

Conceptualization: Jei Hee Lee, Dakeun Lee.
Data curation: Bohyun Kim, Young Bae Kim.
Formal analysis: Jei Hee Lee, Young Bae Kim, Dakeun Lee.
Investigation: Hye Jin Kim, Dakeun Lee.
Methodology: Hye Jin Kim.
Resources: Young Bae Kim, Dakeun Lee.
Supervision: Jai Keun Kim, Young Bae Kim.
Writing – original draft: Bohyun Kim.
Writing – review & editing: Bohyun Kim, Jei Hee Lee.

References

[1] Lee JM, Zech CJ, Bolondi L, et al. Consensus report of the 4th International Forum for Gadolinium-Ethoxybenzyl-Diethylenetriamine Pentaacetic Acid Magnetic Resonance Imaging. Korean J Radiol 2011;12:403–15.
[2] El-Serag HB. Hepatocellular carcinoma. N Engl J Med 2011;365: 1118–27.
[3] Bruix J, Sherman M. Management of hepatocellular carcinoma: an update. Hepatology 2011;53:1020–2.
[4] Ng IO, Lai EC, Ng MM, et al. Tumor encapsulation in hepatocellular carcinoma. A pathologic study of 189 cases. Cancer 1992;70:45–9.
[5] Ishigami K, Yoshimitsu K, Nishihara Y, et al. Hepatocellular carcinoma with a pseudocapsule on gadolinium-enhanced MR images: correlation with histopathologic findings. Radiology 2009;250:435–43.
[6] Grazioli L, Olivetti L, Fugazzola C, et al. The pseudocapsule in hepatocellular carcinoma: correlation between dynamic MR imaging and pathology. Eur Radiol 1999;9:62–7.
[7] Ehman EC, Behr SC, Umetsu SE, et al. Rate of observation and inter-observer agreement for LI-RADS major features at CT and MRI in 184 pathology proven hepatocellular carcinomas. Abdom Radiol 2016;41: 963–9.
[8] Dioguardi Burgio M, Picone D, Cabibbo G, et al. MR-imaging features of hepatocellular carcinoma capsule appearance in cirrhotic liver: comparison of gadoxetic acid and gadobenate dimeglumine. Abdom Radiol 2016;41:1546–54.
[9] Ringe KI, Husarik DB, Sirlin CB, et al. Gadoxetate disodium-enhanced MRI of the liver: part 1, protocol optimization and lesion appearance in the noncirrhotic liver. AJR Am J Roentgenol 2010;195:13–28.
[10] Doo KW, Lee CH, Choi JW, et al. "Pseudo washout" sign in high-flow hepatic hemangioma on gadoxetic acid contrast-enhanced MRI mimicking hypervascular tumor. AJR Am J Roentgenol 2009;193: W490–6.
[11] Chernyak V, Flusberg M, Law A, et al. Liver imaging reporting and data system: discordance between computed tomography and gadoxetate-enhanced magnetic resonance imaging for detection of hepatocellular carcinoma major features. J Comput Assist Tomogr 2017;42:155–61.
[12] Santillan C, Fowler K, Kono Y, et al. LI-RADS major features: CT, MRI with extracellular agents, and MRI with hepatobiliary agents. Abdom Radiol 2017;43:75–81.
[13] An C, Rhee H, Han K, et al. Added value of smooth hypointense rim in the hepatobiliary phase of gadoxetic acid-enhanced MRI in identifying tumour capsule and diagnosing hepatocellular carcinoma. Eur Radiol 2017;27:2610–8.
[14] Elsayes KM, Hooker JC, Agrons MM, et al. 2017 Version of LI-RADS for CT and MR imaging: an update. Radiographics 2017;37: 1994–2017.
[15] Cho ES, Choi JY. MRI features of hepatocellular carcinoma related to biologic behavior. Korean J Radiol 2015;16:449–64.
[16] Nakashima Y, Nakashima O, Tanaka M, et al. Portal vein invasion and intrahepatic micrometastasis in small hepatocellular carcinoma by gross type. Hepatol Res 2003;26:142–7.
[17] Lim JH, Choi D, Park CK, et al. Encapsulated hepatocellular carcinoma: CT-pathologic correlations. Eur Radiol 2006;16:2326–33.
[18] Rimola J, Forner A, Tremosini S, et al. Non-invasive diagnosis of hepatocellular carcinoma $\leq$2 cm in cirrhosis. Diagnostic accuracy assessing fat, capsule and signal intensity at dynamic MRI. J Hepatol 2012;56:1317–23.
[19] Khan AS, Hussain HK, Johnson TD, et al. Value of delayed hypointensity and delayed enhancing rim in magnetic resonance imaging diagnosis of small hepatocellular carcinoma in the cirrhotic liver. J Magn Reson Imaging 2010;32:360–6.
[20] Torimura T, Ueno T, Inuzuka S, et al. Mechanism of fibrous capsule formation surrounding hepatocellular carcinoma. Immunohistochemical study. Arch Pathol Lab Med 1991;115:365–71.
[21] Gressner AM, Weiskirchen R. Modern pathogenetic concepts of liver fibrosis suggest stellate cells and TGF-beta as major players and therapeutic targets. J Cell Mol Med 2006;10:76–99.
[22] Motosugi U, Ichikawa T, Sou H, et al. Liver parenchymal enhancement of hepatocyte-phase images in Gd-EOB-DTPA-enhanced MR imaging: which biological markers of the liver function affect the enhancement? J Magn Reson Imaging 2009;30:1042–6.
[23] Kim YN, Song JS, Moon WS, et al. Intra-individual comparison of hepatocellular carcinoma imaging features on contrast-enhanced computed tomography, gadopentetate dimeglumine-enhanced MRI, and gadoxetic acid-enhanced MRI. Acta Radiol 2017;59:639–48.
[24] Zhang YD, Zhu FP, Xu X, et al. Liver imaging reporting and data system: substantial discordance between CT and MR for imaging classification of hepatic nodules. Acad Radiol 2016;23:344–52.
[25] Joo I, Lee JM, Lee DH, et al. Liver imaging reporting and data system v2014 categorization of hepatocellular carcinoma on gadoxetic acid-enhanced MRI: comparison with multiphasic multidetector computed tomography. J Magn Reson Imaging 2017;45:731–40.
[26] Hope TA, Aslam R, Weinstein S, et al. Change in liver imaging reporting and data system characterization of focal liver lesions using gadoxetate disodium magnetic resonance imaging compared with contrast-enhanced computed tomography. J Comput Assist Tomogr 2017;41:376–81.
[27] Davenport MS, Khalatbari S, Liu PS, et al. Repeatability of diagnostic features and scoring systems for hepatocellular carcinoma by using MR imaging. Radiology 2014;272:132–42.
[28] Hope TA, Fowler KJ, Sirlin CB, et al. Hepatobiliary agents and their role in LI-RADS. Abdom Imaging 2015;40:613–25.
[29] Sofue K, Sirlin CB, Allen BC, et al. How reader perception of capsule affects interpretation of washout in hypervascular liver nodules in patients at risk for hepatocellular carcinoma. J Magn Reson Imaging 2016;43:1337–45.